SPARK PLASMA SINTERING OF BALL MILLED AND ATOMIZED POWDER BASED ON FE-AL

ŠÍMA Vladimír[1], MINÁRIK Peter[1], CHRÁSKA Tomáš[2]

[1]*Charles University in Prague, Prague, Czech Republic, EU*
[2] *Institute of Plasma Physics of the AS CR, v.v.i., Prague, Czech Republic, EU*

Abstract

High-quality compacts were prepared using the spark plasma sintering (SPS) method from powders of similar composition Fe-Al-Zr-B. The properties of the sintered compacts are strongly dependent on the morphology and properties of the feedstock powder. The first powder was obtained by ball milling of the as cast alloy and the second was prepared by atomization under argon atmosphere. The morphology and structure of the two powders are compared and mechanical properties and microstructure of compacts prepared under the same conditions of the SPS procedure are discussed. The milled powder has an irregular morphology and shape of the polycrystalline particles, which have a completely disordered BCC structure with considerable internal stresses, high concentration of structural defects and the presence of aluminum oxide. The atomized powder particles are nearly spherical, polycrystalline with ordered B2 structure, with no significant signs of internal stresses and oxidation. Microhardness of particles of both powders was measured and compared with the microhardness of compact materials, the results of compression tests of compacts at room temperature were compared and discussed.

Keywords: iron aluminides, spark plasma sintering, metallic powders, mechanical properties, microstructure.

1. INTRODUCTION

The FeAl-based intermetallics are attractive materials for appropriate applications at medium to high temperatures mainly due to their low density, low cost as well as excellent oxidation and sulfidation resistance in harsh and corrosive environments [1]. However, their use has been limited by their brittleness at room temperature and poor creep resistance. These drawbacks can be improved by grain boundary and dispersion strengthening as well as grain size reduction. Powder metallurgy techniques such as gas atomization and mechanical milling have been used to develop an oxide (Y_2O_3 particles 20-30 nm in size) dispersion strengthened (ODS) material named FeAl40 Grade 3. The material has been developed initially for consolidation by hot extrusion, now is available in various forming states (forged and rolled plates, swaged and extruded bars, etc.) [2]. The yield strength and the elongation of such alloys can reach at room temperature 900 MPa and 6.4% in air [3]. The high strength has been attributed to the nearly equal contribution of solution hardening of the matrix, fine grain hardening as well as oxide dispersion hardening [4]. The conventional hot extrusion performed at temperatures above 1000 ^oC, inevitably results in grain growth up to the micrometer scale [5].

Spark plasma sintering (SPS) is a consolidation technique involving the simultaneous application of current and pressure. When SPS is applied to powders, densification can be achieved at significantly lower temperatures and shorter times than conventional sintering, thereby limiting grain growth and preserving the microstructure [6].

The present study was undertaken in order to compare properties of the dense fine grained material sintered from the feedstock powder prepared by ball milling [7] with properties of a new material of similar composition, sintered from the feedstock powder prepared by atomization. Microstructure of sintered

samples was characterized by X-ray diffraction (XRD) and scanning electron microscopy with electron back scatter diffraction (EBSD), mechanical properties at room temperature were studied by microhardness and compression tests.

2. EXPERIMENTAL PROCEDURES

The initial alloy (nominal composition Fe-40Al-0.1Zr-0.1B at.%) was prepared by arc melting under pure Ar atmosphere. The purities of materials were Fe: 99.97, Al: 99.9, Zr: 99.95, and B: 99.5 (supplied from Alfa Aeser). The charge materials were melted in a copper crucible cooled by water and then cast in a steel mold (8 mm in diameter). To prevent oxidation, the furnace was evacuated to about 5 Pa and then filled with Ar. The alloy was crushed manually with a hammer into pieces smaller than 10 mm. These pieces were milled in a planetary ball milling machine (Fritsch Pulverisette 5) under Ar atmosphere using hardened steel balls and bowl without a process control agent. The powder was sieved into final size fraction <20 μm [7].

Atomized powder was prepared by LERMPS/PERSEE, France, using atomization in argon. Particle size distribution can be characterized by d_{10} = 13.7 μm, d_{50} = 29.0 μm, d_{90} = 51.2 μm values obtained by laser granulometry.

The powder was consolidated using SPS 10-4 apparatus (Thermal Technology LLC). The graphite die, 20 mm in diameter, loaded with the powder, was heated up in two steps to a sintering temperature of 1100 °C with a heating rate of 200 K/min (compare e.g. with [8]). The first step was a pre-pressing of the powder with a pressure of 5 MPa followed by evacuation of the chamber to 5 Pa and heating to 450 °C. A pressure of 60 MPa was applied at this temperature and maintained until completion of sintering. The dwell time at 1100 °C was 70 s, followed by fast cooling (200 K/min) to 850 °C and then by slower cooling (100 K/min) to room temperature. The dimensions of the end-product were about Ø19 mm x 5 mm.

XRD measurements were performed on the milled powder and the sintered bulk sample using a Bragg Brentano θ/2θ Bruker X-ray diffractometer, type D8 (Cu K_α radiation, λ = 0.15418 nm).

The chemical analysis of Al, B, Cr, Fe, Ni, Zr was performed by ICP-OES method using Iris Intrepid HR, Thermo Scientific, the analysis of C was made using absorption spectrometer LECO CS-444, the analysis of O was made using absorption spectrometer LECO TC-300.

Microhardness measurements were performed on powder particles and on compacted samples using Qness Q10A microhardness tester with Vickers loads ranging from 2.5 gram to 500 gram.

Cuboid-shaped compressive samples, 4.94 x 3.47 x 3.66 mm^3, were sectioned by diamond saw from the SPS disk. Uniaxial compressive tests were performed in air at room temperature with an initial strain rate of 1.0 x 10^{-4} s^{-1}, using an Instron 1186 universal testing machine.

The microstructure of the SPS-consolidated bulk sample was examined by scanning electron microscopy and transmission electron microscopy. SEM observations were performed using Zeiss Auriga Compact Crossbeam® (FEG + FIB) microscope equipped with EDAX EBSD camera DigiView 5.

3. RESULTS

3.1. XRD analysis of powders and sintered bulk samples

XRD pattern of the milled powder confirmed the presence of a single phase structure of disordered bcc-phase with a = 0.2919(1) nm, the broadening of XRD peaks indicated an effect of crystallite size reduction and also straining of powder particles during milling process [7].

XRD pattern of the sample sintered from milled powder showed a more complex phase composition. Due to the nominal composition of 40 at.% Al the ordering process in the sintered material should result in the B2

structure of the matrix. The diffraction pattern consisted not only from peaks of the B2 structure with a = 0.28927(5) nm, there are also superlattice reflections indicating $D0_3$ structure (Fe_3Al) with a = 0.5781(5) nm, peaks from κ-$Fe_3AlC_{0.5}$ carbide with a = 0.3743(2) nm and small, probably α-Al_2O_3 (corundum) peaks corresponding a = 0.4754(5) nm, c = 1.2990(5) nm [7]. This indicated that formation of all these phases has occurred during the SPS process, the presence of carbon was clarified by chemical analysis of the powder and the sintered sample, carbon was contained in the milled powder - see below.

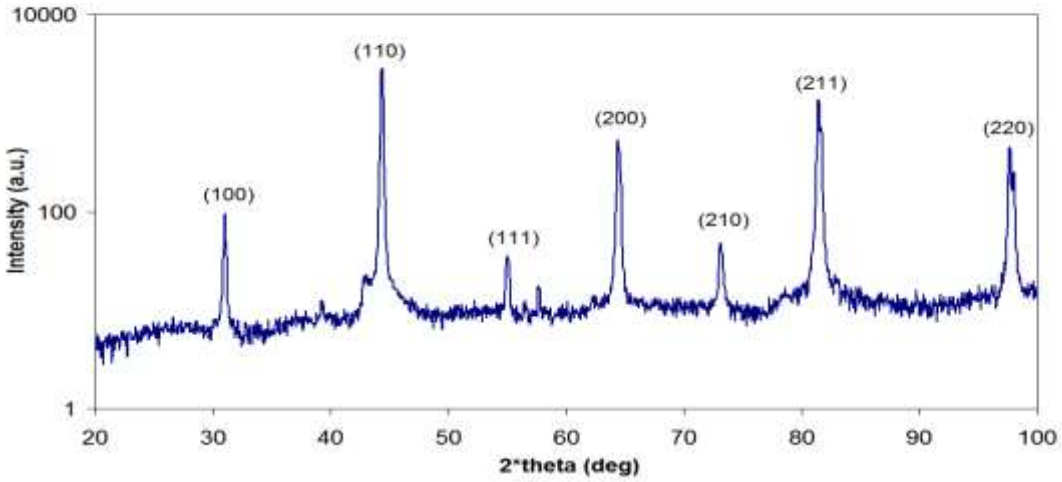

Fig. 1 XRD pattern of the as-received atomized powder, diffraction peaks correspond to the B2 structure with a = 0.2896(1) nm.

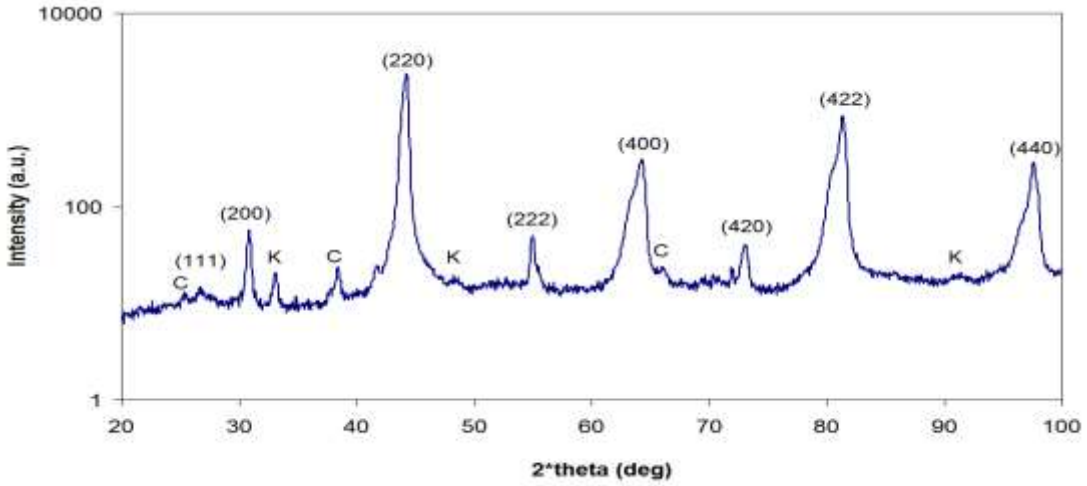

Fig. 2 XRD pattern of the sample sintered from atomized powder. The peaks with indices are peaks of $D0_3$ structure with a = 0.5795(3) nm, peaks denoted by *K* correspond to the κ-$Fe_3AlC_{0.5}$ carbide with a = 0.3743(2) nm, peaks of corundum with a = 0.4754(5) nm, c = 1.2990(5) nm are denoted by *C*.

XRD pattern of the as-received atomized powder is presented in **Fig. 1** and confirms the presence of the ordered B2 phase. There are not clear signs of the transformation into $D0_3$ structure in spite of ferromagnetic behavior of the powder at room temperature. XRD measurement performed after the annealing 408 h/420 °C

of the powder in argon clearly showed the fully evolved $D0_3$ equilibrium structure with fcc Bravais lattice and doubled lattice parameter of a = 0.57914(2) nm.

XRD pattern of the sample sintered from atomized powder is presented in **Fig. 2**. The diffraction pattern in **Fig. 2** consists not only from peaks of the B2 structure, there is also the (111) superlattice reflection indicating $D0_3$ structure (Fe_3Al) and peaks from κ-$Fe_3AlC_{0.5}$ carbide and α-Al_2O_3 (corundum). The further formation of the $D0_3$ structure in the sintered sample was confirmed by the XRD measurements, performed after annealing 408 h/420 °C in argon. The formation of the κ-phase and corundum occurred, similarly as in case of milled powder, during the SPS process. The carbon in this case comes from graphite foil surrounding the sample during the SPS process – see below.

3.2. Chemical analysis of powders and sintered bulk samples

The chemical composition of both feedstock powders is displayed in **Table 1**.

Table 1 Chemical composition (at.%) of powders

element	Fe	Al	B	C	Cr	Ni	O	Zr
milled powder	60.9	36.3	0.02	0.56	0.25	0.27	1.00	0.08
atomized powder	68.5	30.8	0.11	0.06	0.00	0.00	0.13	0.35

The chemical analysis of C and Al was made also for the sample sintered from milled powder, the content of both elements was the same as in the feedstock powder [7]. It means that carbon (and also chromium and nickel) comes from the stainless-steel balls and bowl in the milling procedure. The κ-phase, observed in the sample sintered from atomized powder, was formed during the SPS by diffusion of carbon into sample from graphite foil and graphite die of the SPS apparatus.

3.3. Mechanical properties of powders and sintered bulk samples

The mechanical properties of powders were characterized by microhardness measurements on individual powder particles, the same measurements were performed also on sintered samples – see **Table 2**.

Table 2 Microhardness HV 0.025 of powder particles and sintered materials, 0.2% offset yield strength of sintered materials at room temperature

	HV 0.025	0.2% offset yield strength [MPa]
milled powder	800 ± 90	-
SPS bulk from milled powder	790 ± 60	1325
atomized powder	380 ± 20	-
SPS bulk from atomized powder	370 ± 15	630

The 0.2% offset yield strength values, obtained from compression tests on sintered materials at room temperature with an initial strain rate of 1.0×10^{-4} s^{-1}, are summarized in **Table 2** too. It can be seen that the yield strength values of compacted materials are proportional to their microhardness values which are determined by microhardness of feedstock powder particles.

3.4. Microstructure of powder particles and sintered bulk samples

Using optical metallography methods did not enable to visualize the microstructure of the sintered materials, we did not observe also any signs of a porosity of the bulk. The density measurement (Archimedes method) of the sintered material gave the relative density higher than 99% [7].

The identification and visualization of grains of the matrix and also of the κ-$Fe_3AlC_{0.5}$ carbide was made using of the EBSD method for the material sintered from milled powder [7]. The average grain size was d = (1.6 ± 0.6) μm, the estimated partition fraction of the κ-$Fe_3AlC_{0.5}$ carbide was lower than about 20% [7]. In case of atomized powder we succeeded also in determination of microstructure of individual powder particles which have nearly perfect spherical form - see **Fig. 3**.

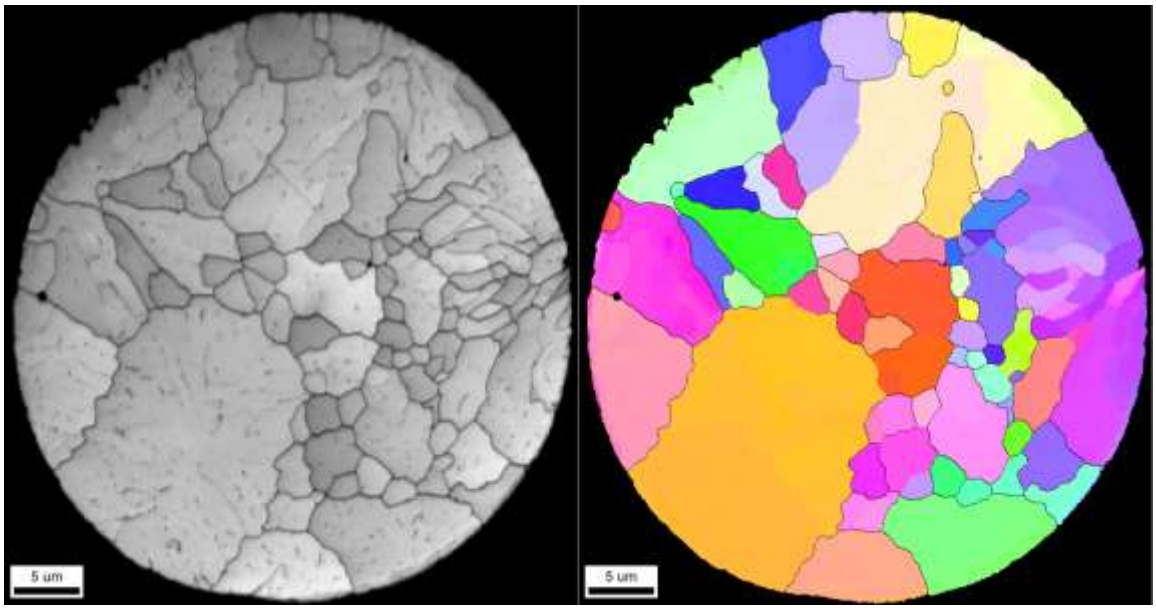

Fig. 3 Example of microstructure of atomized powder particle observed by SEM and EBSD method.

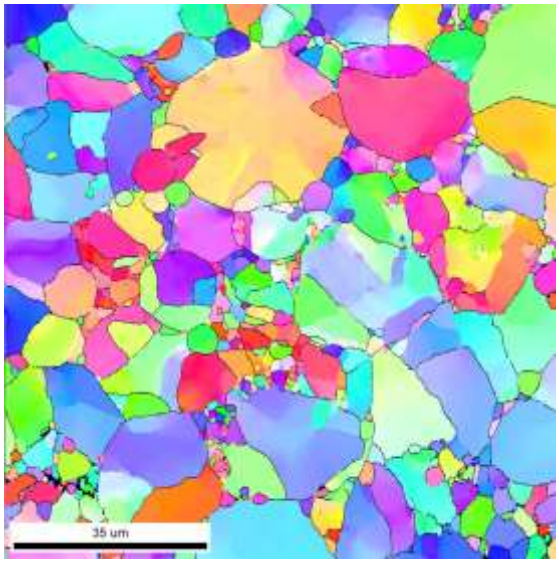

Fig. 4 Example of microstructure of the material sintered from atomized powder observed by EBSD method.

The microstructure of the material sintered from atomized powder (**Fig. 4**) is determined by the microstructure of atomized particles, i.e. in the sintered bulk there are very similar grains as in powder

particles, additionally there are also some new fine grains grown during sintering process. The resulting microstructure has therefore a bimodal or multimodal distribution of grain sizes.

4. DISCUSSION

The usual way of preparation of a feedstock powder for the SPS is the atomimization of an alloy or a mechanical alloying of elemental powders by mechanical milling or cryomilling.

In this work we compare some properties of materials sintered from completely disordered and heavily strained powder and from long range ordered atomized powder of similar compositions. It seems that mechanical properties of both different sintered materials at room temperature are not significantly influenced by differences in secondary contamination by O, C, Cr, Ni, the microhardness and yield strength of sintered materials is probably driven by a combination of strain hardening and fine grain hardening, determining differences in microhardness of feedstock powder particles and persisting also in sintered material. The systematic investigation of such an effect will be based on cryomilling of the same atomized powder. The variable time and intensity of milling will result in various straining of the feedstock powder particles and this way we are going to influence the mechanical properties of sintered material.

CONCLUSION

This work examined and compared the microstructure and mechanical properties of two materials obtained by SPS from two feedstock powders of similar composition prepared by mechanical milling and by atomization. The results of performed experiments show a key role of straining of feedstock powder particles for the mechanical properties of materials prepared by the SPS process.

ACKNOWLEDGEMENTS

This research was supported by the Czech Science Foundation, project No. 15-15609S.

REFERENCES

[1] DEEVI S.C., SIKKA V.K. Nickel and Iron Aluminides: An Overview on Properties, Processing, and Applications. Intermetallics, Vol. 4, 1996, pp. 357-375.

[2] REVOL S., BACCINO R., MORET F. Industrial Applications of FeAl40 Grade3, a high specific properties Iron Aluminide. In Euromat99, Munich, FRG, Ed. D.G. Morris, S. Naka, and P. Caron. Wiley-CH, 1999, pp. 307-311.

[3] MORET F. et al. Propriétés et applications des alliages intermétalliques B2-FeAl. J. Phys. IV France, Vol. 6, 1996, pp. C2-281-C2-289.

[4] MUÑOZ-MORRIS M.A., OCA C.G., MORRIS D.G. Microstructure and Room Temperature Strength of Fe-40Al Containing Nanocrystalline Oxide Particles. Acta Mater., Vol. 51, 2003, pp.5187-5197.

[5] MORRIS D.G, GUNTHER S. Strength and Ductility of Fe-40Al Alloy Prepared by Mechanical Alloying. Mater., Sci. Eng. A, Vol. 208, 1996, pp. 7-19.

[6] ORRU R. et al. Consolidation/Synthesis of Materials by Electric Current Activated/Assisted Sintering. Mater. Sci. Eng. R, Vol. 63, 2009, pp. 127-287.

[7] ŠÍMA V., CIESLAR M., ÇELIKYÜREK I., TORUN O., CHRÁSKA T. Fully Dense Fine Grained FeAl-based Intermetallics Prepared by Spark Plasma Sintering Method. In Proceedings of the 8th Pacific Rim International Congress on Advanced Materials and Processing (PRICM8), editor: Fernand Marquis, Wiley, 2013, pp. 361-368.

[8] SKIBA T. et al. Mechanical Properties of Spark Plasma Sintered FeAl Intermetallics. Intermetallics, Vol. 18, 2010, pp. 1410-1414